Pergamon

Int. J. Solids Structures Vol. 32, No. 3/4, pp. 315–328, 1995

0020–7683/95 $9.50 + .00

0020–7683(94)00154–5

FIBER–MATRIX DEBONDING EFFECTS ON CRACKING IN ALIGNED FIBER CERAMIC COMPOSITES

B. BUDIANSKY, A. G. EVANS† and J. W. HUTCHINSON
Division of Applied Sciences, Harvard University, Cambridge, MA 02138, U.S.A. and
†Materials Department, University of California, Santa Barbara, CA 93106, U.S.A.

(*Received* 12 *July* 1994)

Abstract—The micromechanical fracture analysis of fiber-reinforced ceramics usually requires explicit consideration of sliding at the fiber–matrix interface that is resisted by frictional shear stress. But an interfacial debonding resistance may have to be overcome before frictional sliding can occur. This paper presents an approximate calculation of the stresses needed to initiate and propagate fiber–matrix debonding in the vicinity of a matrix crack. The results are used to define the parameters of a crack-bridging model that serves to determine the effects of debonding and initial stress on the matrix cracking stress of an aligned fiber composite, as well as their effects on overall composite toughness.

1. INTRODUCTION

Matrix cracks bridged by intact reinforcing fibers are commonplace in ceramic fiber composites. The micromechanical analysis of crack-bridging fibers is essential in order to incorporate their effects into the study of the constitutive behavior and fracture of aligned fiber composites, or aligned fiber layers within composite laminates. A widely used assumption is that the fibers are held in the matrix solely by the presence of friction, and that axial sliding along a fiber–matrix interface would occur under a critical, limiting value of longitudinal shear stress. This assumption, together with some additional simplifications, underlies the classical Aveston–Cooper–Kelly (ACK) *matrix cracking stress* [Aveston *et al.* (1971); see also Budiansky *et al.* (1986); McCartney (1987)] and also recent results for the strength of an aligned fiber composite containing an initial through-the-fiber flaw (Budiansky and Cui, 1994).

In the present paper we extend the traditional modeling of frictionally sliding fibers to include the effect of a debonding *toughness* at the fiber–matrix interface that must be overcome before sliding can occur. In so doing, we are guided by the approach of Hutchinson and Jensen (1990), who overlaid the influence of interface toughness on an unconventional frictional sliding model, that in some respects is more elaborate than earlier ones. Here we retain the constant friction, shear-lag model of Budiansky *et al.* (1986) as the starting point for building in the interface toughness effect. A popular and convenient way to embody the mechanical effects on a composite of crack-bridging fibers is to introduce a continuous distribution of non-linear springs that connect the opposing faces of a crack in a homogeneous material. In this idealization, the spring law relating stress and displacement is chosen so as to reproduce the overall tensile compliance of the prototype composite material when it is fully traversed by a bridged matrix crack. Accordingly, we derive an equivalent crack-bridging spring law that includes the influence of debonding toughness as well as friction. We then go on to find results for the increase in the matrix cracking stress produced by the introduction of debonding toughness. Finally, we give an estimate for the effect of debonding toughness on the tensile strength of a composite containing a long through-fiber flaw. Here the result is a strength *reduction*, but generally a small one.

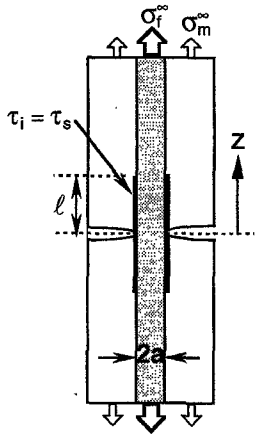

Fig. 1. Fiber and matrix.

2. SHEAR-LAG MODELS AND BRIDGING LAWS

2.1. *Stress analysis*

We contemplate an aligned fiber composite under tension containing a long matrix crack normal to the fiber direction, and analyse the fiber–matrix interaction on the basis of a single composite cylinder (Fig. 1). The fiber of radius a is assumed to maintain radial contact with the surrounding matrix cylinder, whose outer radius is chosen to give the right fiber and matrix volume concentrations c_f and $c_m = 1 - c_f$. The lateral sides of the matrix cylinder are assumed traction free, and a uniform axial strain is imposed at $z = \infty$, producing the far-field, average fiber and matrix stresses σ_f^∞ and σ_m^∞. Thus the average composite stress $\sigma = c_f\sigma_f^\infty + c_m\sigma_m^\infty$ is resisted by the fiber stress σ/c_f at the matrix crack. Axial sliding occurs at the fiber–matrix interface in the interval $0 < z < \ell$, where the longitudinal shear stress is equal to a limiting frictional stress τ_s. The magnitude of ℓ, which could be zero, will come out from the solution. The fiber and matrix Young's moduli are E_f and E_m, the composite Young's modulus is $E = c_fE_f + c_mE_m$, and the far-field strain is $\sigma/E = \sigma_f^\infty/E_f = \sigma_m^\infty/E_m$. Poisson's ratio effects are ignored in these last two equations. Finally, for simplicity of exposition, we postpone consideration of initial stress, which can be handled efficiently after we look at the combined effects of frictional shear resistance and debonding toughness.

According to the shear-lag solution given by Budiansky *et al.* (1986), the average fiber and matrix tensile stresses $\sigma_f(z)$ and $\sigma_m(z)$, and the interface shear stress $\tau_i(z)$ are given by

$$\begin{aligned} \sigma_f(z) &= \sigma/c_f - 2\tau_s z/a \\ \sigma_m(z) &= (2c_f/c_m)\tau_s z/a \\ \tau_i(z) &= \tau_s \end{aligned} \tag{1}$$

for $0 < z < \ell$, and by

$$\begin{aligned} \sigma_f(z) &= \sigma_f^\infty + [(c_m/c_f)\sigma_m^\infty - 2\tau_s\ell/a]\, e^{-\rho(z-\ell)/a} \\ \sigma_m(z) &= \sigma_m^\infty - [\sigma_m^\infty - (2c_f/c_m)\tau_s\ell/a]\, e^{-\rho(z-\ell)/a} \\ \tau_i(z) &= (\rho/2)[(c_m/c_f)\sigma_m^\infty - 2\tau_s\ell/a]\, e^{-\rho(z-\ell)/a} \end{aligned} \tag{2}$$

for $z > \ell$. The shear-lag parameter ρ is defined by

$$\rho = \frac{B^2}{c_m}\left[\frac{6E}{E_f(1+\nu_m)}\right]^{1/2} \tag{3}$$

where ν_m is the Poisson's ratio of the matrix, and where the utility constant B is given by

$$B = \left[\frac{2c_m^3}{-6\log c_f - 3c_m(3-c_f)}\right]^{1/4} \tag{4}$$

(for $c_f = 0.4$, B ≈ 0.85; for $c_f \to 1$, $B \to 1$). The tensile stresses given by eqns (1, 2) are continuous at $z = \ell$, but not necessarily the interface shear stress.

2.2. *Zero interface toughness; spring bridging law*

If the debonding energy release rate $\mathcal{G}_D$ of the fiber–matrix interface vanishes, ℓ will remain equal to zero until the interface shear stress at $z = 0$ reaches τ_S. This will happen when the applied stress σ becomes equal to the critical value

$$\sigma_S = \left(\frac{2c_f E}{c_m E_m}\right)\frac{\tau_S}{\rho}. \tag{5}$$

For $\sigma > \sigma_S$ the sliding length ℓ is set by the condition of interface shear continuity at $z = \ell$, and is given by

$$\ell/a = \left(\frac{c_m E_m}{c_f E}\right)\frac{\sigma}{2\tau_S} - \frac{1}{\rho}. \tag{6}$$

The second term is usually quite small, less than unity. Note that we can rewrite eqn (6) as

$$\ell/a = \left(\frac{c_m E_m}{c_f E}\right)\frac{\sigma - \sigma_S}{2\tau_S} \tag{7}$$

for $\sigma > \sigma_S$.

A spring bridging law can now be formulated by application of the approach introduced by Hutchinson and Jensen (1990). The matrix-cracked composite (see Fig. 2) is stretched uniformly at $z = \pm L$ by an average stress σ, and the same stress is applied to the spring model, which consists of two homogeneous slabs having the composite modulus E, and connected by springs that stretch an amount $2v$. For equality of the end displacements W in model and prototype, the spring stretch must satisfy

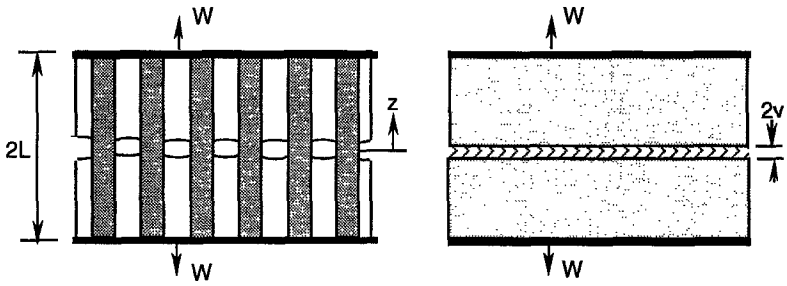

Fig. 2. Fiber bridging prototype and spring model; the average applied stress is σ.

$$v = \int_0^L \frac{\sigma_f(z)}{E_f} dz - \frac{\sigma L}{E}. \tag{8}$$

Letting $L \to \infty$, and substituting $\sigma_f(z)$ from eqn (1), with ℓ specified by eqn (7), leads to the bridging law

$$\frac{v}{a} = 2\left(\frac{\sigma_S}{\sigma_A}\right)\left(\frac{\sigma}{\sigma_A}\right) \quad \text{for } \sigma < \sigma_S \tag{9a}$$

$$= \left(\frac{\sigma}{\sigma_A}\right)^2 + \left(\frac{\sigma_S}{\sigma_A}\right)^2 \quad \text{for } \sigma > \sigma_S \tag{9b}$$

where σ_A is a reference stress defined by

$$\sigma_A = \frac{2c_f E\sqrt{E_f \tau_S}}{c_m E_m}. \tag{10}$$

To compare with earlier studies, we note that the spring relations given in eqns (9) are identical with those exhibited in a different notation by Marshall and Cox (1988) and Budiansky and Amazigo (1989). They are fully consistent with the energy analysis of matrix cracking presented by Budiansky *et al.* (1986), which covered the full range of frictional resistance τ_S. The classical Aveston–Cooper–Kelly theory (Aveston *et al.*, 1971) for matrix cracking in the presence of frictionally sliding fibers incorporated the widely used "large slip" assumption, in which the $1/\rho$ term in eqn (6) for the slip length ℓ is dropped, and all deformations associated with the exponentially decaying stress contributions in eqns (2) are ignored. This is equivalent to dropping the σ_S terms in the spring relations [eqns (9)], which gives the quadratic bridging law

$$\frac{v}{a} = \left(\frac{\sigma}{\sigma_A}\right)^2 \tag{11}$$

for all values of σ. While this simplified spring law appears to be quite adequate when interface sliding is resisted only by realistic magnitudes of constant friction, it will be necessary to build on to the more accurate relations in eqns (9) when we introduce the effects of debonding toughness.

2.3. *Non-zero debonding energy; spring bridging law*

We now seek to incorporate the influence of a debonding toughness into our shear-lag analysis, following the scheme that was used by Hutchinson and Jensen (1990). (We note, in passing, that in the sliding region adjacent to the matrix crack, the shear-lag model of Hutchinson and Jensen is more sophisticated than the present one, but in the spirit of the large slip approximation, they ignore the details of the exponential decay zone.) Although radial stresses do not enter into our analysis, we will assume that radial displacement continuity is maintained in the sliding regime, so that the condition for mode II debonding must be met for propagation of the sliding boundary. We first contemplate the composite-cylinder configuration shown in Fig. 3, wherein a very long, *zero friction*, debonded zone

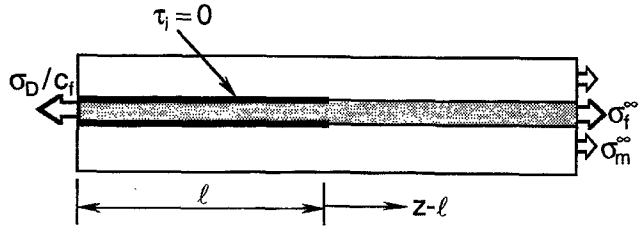

Fig. 3. Zero friction debonding; average stress is σ_D at $z = \infty$.

is propagating under a critical value σ_D of the average applied stress σ at $z = \infty$. An elementary energy release calculation gives

$$\sigma_D = 2c_f \sqrt{\frac{E_f E \mathscr{G}_D}{c_m E_m a}} \tag{12}$$

for this debonding stress in terms of the critical energy release rate $\mathscr{G}_D$ for mode II interface debonding. Except for the neglect of Poisson's ratio effects, this is an exact three-dimensional result, but now we will use it in an approximate fashion to modify the shear-lag theory to take debonding toughness into account. The shear-lag approximation to the stresses in $(z-\ell) > 0$ (Fig. 3) is given by eqns (2) with $\tau_S = 0$, and so the interface shear stress $\tau_i(z)$ at $z = \ell^+$, just beyond the tip of the zero friction interface crack is

$$\tau_i(\ell^+) = \left(\frac{c_m \rho}{2c_f}\right)\sigma_m^\infty. \tag{13}$$

Of course, the three-dimensional shear stress is singular at $z = \ell^+$, but within the framework of shear-lag theory, it makes sense to set $\sigma_m^\infty = (E_m/E)\sigma_D$ in eqn (13) in order to define a critical interface shear stress τ_D required for debonding as

$$\tau_D = \left(\frac{\rho c_m E_m}{2c_f E}\right)\sigma_D. \tag{14}$$

We think of τ_D as a cohesive shear strength of the interface that may not be exceeded by the shear stress $\tau_i(z)$. Hence, in our shear-lag theory, the value of σ_D given by eqn (12) represents the critical applied stress for continued debonding of a zero friction sliding zone of *arbitrary* length ℓ.

To establish a general criterion for continued interface debonding (see Fig. 1) in the presence of sliding friction τ_S along a debonded zone of arbitrary length ℓ, we take the decisive step of postulating the condition

$$\tau_i(\ell^+) = \max\begin{pmatrix}\tau_D \\ \tau_S\end{pmatrix}. \tag{15}$$

The idea is this: in our shear-lag theory, wherever interface sliding occurs $\tau_i(z) = \tau_S$, so if $\tau_D < \tau_i(\ell^+) < \tau_S$, extension of the debonded zone is prevented by friction, even though τ_i is sufficiently high to overcome the cohesive resistance τ_D of the interface. Hence, for $\tau_D < \tau_S$, all of the shear-lag results for zero debonding toughness, as well as the bridging law in eqns (9), continue to apply. But for $\tau_D > \tau_S$ (or equivalently, $\sigma_D > \sigma_S$) there can be no debonding for $\sigma < \sigma_D$ in which case we must have $\ell = 0$. Then, for $\sigma > \sigma_D > \sigma_S$, we may set $\tau_i(\ell^+) = \tau_D$ in eqn (2) in order to calculate the debonding length ℓ, and we find

$$\ell/a = \left(\frac{c_m E_m}{c_f E}\right)\frac{\sigma - \sigma_D}{2\tau_S}. \tag{16}$$

This, of course, is just eqn (7) with σ_S replaced by σ_D, but now the interface shear stress is not a continuous function of z, but jumps from τ_S to τ_D at $z = \ell$. Repeating the calculation of the spring displacement specified by eqn (8) gives, for $\sigma_D > \sigma_S$, the spring law

$$\frac{v}{a} = 2\left(\frac{\sigma_S}{\sigma_A}\right)\left(\frac{\sigma}{\sigma_A}\right) \qquad \text{for } \sigma < \sigma_D \tag{17a}$$

$$= \left(\frac{\sigma}{\sigma_A}\right)^2 - \left(\frac{\sigma_D}{\sigma_A}\right)^2 + 2\left(\frac{\sigma_S}{\sigma_A}\right)\left(\frac{\sigma_D}{\sigma_A}\right) \quad \text{for } \sigma > \sigma_D. \tag{17b}$$

The bridging law still has a continuous slope, and reduces to eqns (9) for $\sigma_S = \sigma_D$.

It may be useful to record a uniformly valid form of the bridging law. Note that according to our shear-lag analysis, the value of the applied stress (Fig. 1) that *initiates* sliding is

$$\sigma_I \equiv \max\left(\frac{\sigma_D}{\sigma_S}\right). \tag{18}$$

It follows that the bridging law may be written as

$$\frac{v}{a} = 2\left(\frac{\sigma_S}{\sigma_A}\right)\left(\frac{\sigma}{\sigma_A}\right) \qquad \text{for } \sigma \leqslant \sigma_I \tag{19a}$$

$$= \left(\frac{\sigma}{\sigma_A}\right)^2 - \left(\frac{\sigma_I}{\sigma_A}\right)^2 + 2\left(\frac{\sigma_S}{\sigma_A}\right)\left(\frac{\sigma_I}{\sigma_A}\right) \quad \text{for } \sigma \geqslant \sigma_I. \tag{19b}$$

These reduce to eqns (9) for $\sigma_D < \sigma_S$, to (17) for $\sigma_D > \sigma_S$, and to both for $\sigma_D = \sigma_S$.

3. MATRIX CRACKING STRESS

3.1. *Calculation via spring complementary energy*

The matrix cracking stress σ_{mc}, defined as the value of the far-field average stress σ needed to propagate a single, long matrix crack through the composite (Fig. 4), is readily found by setting the crack front energy release rate $c_m \mathcal{G}_m$ equal to the rate of potential energy loss in the composite as the crack front advances. Here $\mathcal{G}_m$ is the critical mode I toughness of the matrix material, and the factor c_m takes into account the area reduction due to the fibers. The potential energy calculation is facilitated by use of the spring law $v(\sigma)$ in the spring bridging model (Marshall and Cox, 1988; Budiansky and Amazigo, 1989). Thus the potential energy release per unit crack advance (per unit thickness) is simply

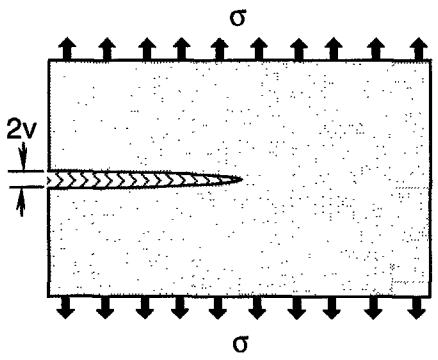

Fig. 4. Long matrix crack propagating under stress σ_{mc}.

$$Q(\sigma) = 2\left[-\int_0^{\sigma} \sigma \, dv(\sigma) + \sigma v(\sigma)\right]$$

$$= 2\int_0^{\sigma} v(\sigma)\, d\sigma. \tag{20}$$

This is actually the complementary energy of the springs, and the matrix cracking stress σ_{mc} satisfies

$$Q(\sigma_{mc}) = c_m \mathscr{G}_m. \tag{21}$$

Equation (20) for the complementary energy embodies the assumption that $\sigma = 0$ at $v = 0$, and will need modification later when we consider initial stresses.

3.2. *Aveston–Cooper–Kelly (ACK) matrix cracking stress*

Using the simplified bridging law [eqn (11)] in eqn (20) leads to the primitive energy expression

$$Q_0(\sigma) = \frac{2}{3}\frac{\sigma^3 a}{\sigma_A^2} \tag{22}$$

and writing

$$Q_0(\sigma_{mc}^0) = c_m \mathscr{G}_m \tag{23}$$

gives the classical matrix cracking stress of Aveston *et al.* (1971)

$$\sigma_{mc}^0 = [(3/2)\sigma_A^2 c_m \mathscr{G}_m]^{1/3} = \left[\frac{6c_f^2 E_f E^2 \tau_S \mathscr{G}_m}{c_m E_m^2 a}\right]^{1/3} \tag{24}$$

for frictionally sliding fibers. We will use this as the baseline quantity with which to compare the results of other calculations. Henceforth, we can use the equivalence

$$Q(\sigma_{mc}) = Q_0(\sigma_{mc}^0) \tag{25}$$

which follows from eqns (21) and (23) to determine other values of the matrix cracking stress σ_{mc}.

3.3. *Matrix cracking stresses of Budiansky–Hutchinson–Evans (BHE)*

The extended results for σ_{mc} found by Budiansky *et al.* (1986) for arbitrary friction magnitudes (but no debonding toughness) follow from the complementary energy functional

$$Q(\sigma) = \frac{2a}{\sigma_A^2}[\sigma_S \sigma^2] \qquad \text{for } \sigma < \sigma_S \tag{26a}$$

$$= \frac{2a}{3\sigma_A^2}[\sigma^3 + 3\sigma\sigma_S^2 - \sigma_S^3] \quad \text{for } \sigma > \sigma_S \tag{26b}$$

obtained by the substitution of eqn (9) into eqn (20). Using eqn (26a) in eqn (25) gives σ_{mc} equal to the "no-slip" matrix cracking stress σ_{ns} defined by

$$\sigma_{ns} \equiv \sqrt{\frac{(\sigma_{mc}^0)^3}{3\sigma_S}} = B\left[\frac{6c_f 2E_f E^3}{c_m^2(1+\nu_m)}\right]^{1/4}\left[\frac{\mathscr{G}_m}{aE_m}\right]^{1/2}. \tag{27}$$

But this equals σ_{mc} only if σ_{ns} is smaller than the critical stress σ_S that produces interface slip. The more usual situation is that $\sigma_S < \sigma_{ns}$, and then σ_{mc} must satisfy the cubic equation

$$\sigma_{mc}^3 + 3\sigma_{mc}\sigma_S^2 - \sigma_S^3 = (\sigma_{mc}^0)^3 \tag{28}$$

deduced from eqns (25) and (26b). The transition between the slip and the no-slip results occurs when eqn (28) is satisfied by $\sigma_{mc} = \sigma_{ns}$; this occurs for $\sigma_{mc} = \sigma_{ns} = (1/3)^{1/3}\sigma_{mc}^0$.

In terms of the non-dimensional ratios

$$\lambda = \frac{\sigma_{mc}}{\sigma_{mc}^0} \quad \text{and} \quad \beta = \frac{\sigma_S}{\sigma_{mc}^0} \tag{29}$$

eqn (28) gives the slipping fiber result

$$\lambda^3 + 3\lambda\beta^2 - \beta^3 = 1 \tag{30}$$

and this provides the solid part of the curve for λ versus β in Fig. 5, valid up to $\lambda = \beta = (1/3)^{1/3} \approx 0.693$. (Note that although λ is a decreasing function of β, σ_{mc} increases with increasing τ_S.) For $\beta > (1/3)^{1/3}$, σ_{mc} stays equal to the no-slip matrix cracking stress σ_{ns}. From the connection

$$\frac{\sigma_S}{\sigma_{mc}^0} = \frac{1}{3}\left(\frac{\sigma_{mc}^0}{\sigma_{ns}}\right)^2 \tag{31a}$$

that follows from eqn (27), we have $\lambda = (3\beta)^{-1/2}$ for $\beta \geqslant (1/3)^{1/3}$, as shown by the "no-slip", dashed part of the curve in Fig. 5. It is commonly thought, however, that in the absence of interface sliding, matrix cracks would tend to propagate dangerously into the fibers. The essential message of Fig. 5 is that in the absence of debonding energy, the ACK σ_{mc}^0 is higher than the BHE matrix cracking stress. However, for the modest values of σ_S/σ_{mc}^0, less than 0.2, that usually apply, the difference is small.

Equation (31a) permits the use of $\sigma_{mc}^0/\sigma_{ns}$ as an alternative non-dimensional measure of the size of the sliding friction. In fact, BHE displayed the results of Fig. 5 in a different manner by plotting σ_{mc}/σ_{ns} versus $\sigma_{mc}^0/\sigma_{ns}$.

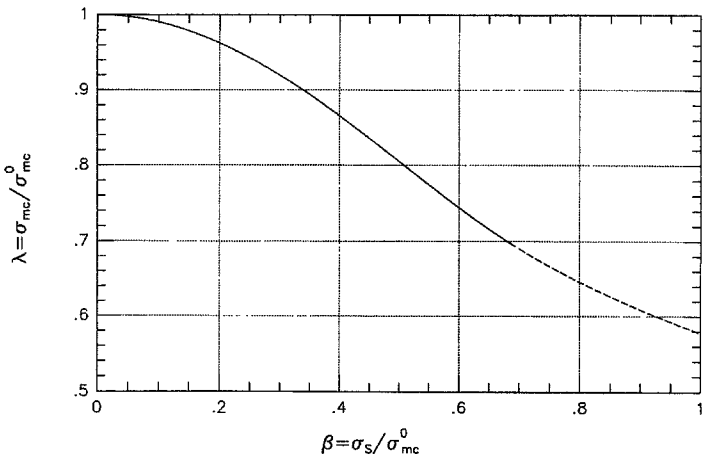

Fig. 5. Effect of friction on matrix cracking stress; $\sigma_{mc} = \sigma_{ns}$ for $\beta \geqslant (1/3)^{1/3} \approx 0.693$.

3.4. *Effect of debonding energy*

For $0 < \sigma_D < \sigma_S$, the BHE results of the previous section continue to apply. To derive the new results required for $\sigma_D > \sigma_S$, we substitute the spring law (17) into eqn (20) for the complementary energy $Q(\sigma)$ to get

$$Q(\sigma) = \frac{2a}{\sigma_A^2}[\sigma_S \sigma^2] \qquad \text{for } \sigma < \sigma_D \tag{31b}$$

$$= \frac{2a}{3\sigma_A^2}[\sigma^3 - 3\sigma\sigma_D(\sigma_D - 2\sigma_S) + \sigma_D^2(2\sigma_D - 3\sigma_S)] \qquad \text{for } \sigma > \sigma_D \tag{31c}$$

and then eqns (25) and (31c) give

$$\sigma_{mc}^3 - 3\sigma_{mc}\sigma_D(\sigma_D - 2\sigma_S) + \sigma_D^2(2\sigma_D - 3\sigma_S) = (\sigma_{mc}^0)^3 \tag{32}$$

for $\sigma_{mc} > \sigma_D$. For increasing σ_D, the transition to the no-slip matrix cracking with $\sigma_{mc} = \sigma_{ns}$ implied by eqn (31a) will occur when eqn (32) is satisfied by $\sigma_{mc} = \sigma_D$; this gives the critical value $\sigma_D = \sqrt{(\sigma_{mc}^0)^3/(3\sigma_S)}$ for no-slip cracking. Introducing

$$\alpha = \frac{\sigma_D}{\sigma_{mc}^0} \tag{33}$$

in addition to the ratios defined in eqn (29), we can now summarize the results of this section for matrix cracking in the presence of both friction and debonding toughness as follows:

$$\lambda^3 + 3\lambda\beta^2 - \beta^3 = 1 \qquad \text{for } \alpha < \beta < (1/3)^{1/3} \tag{34a}$$

$$\lambda^3 - 3\lambda\alpha(\alpha - 2\beta) + \alpha^2(2\alpha - 3\beta) = 1 \qquad \text{for } \beta < \alpha < (3\beta)^{-1/2} \tag{34b}$$

$$\lambda = \frac{\sigma_{ns}}{\sigma_{mc}^0} = (3\beta)^{-1/2} \qquad \text{for } \beta > (1/3)^{1/3} \text{ or } \alpha > (3\beta)^{-1/2}. \tag{34c}$$

Where the cubic equation (34b) for λ has more than one real root, only the largest one is physically meaningful; the others correspond to either negative v or negative σ.

Figure 6 shows examples of λ versus α for three values of β, namely $\beta = 1/12$, corresponding to $\sigma_{ns}/\sigma_{mc}^0 = 2$, $\beta = 0 (\sigma_{ns}/\sigma_{mc}^0 = \infty)$ and $\beta = (1/3)^{1/3} (\sigma_{ns}/\sigma_{mc}^0 = (1/3)^{1/3})$. Also, the solid curve of Fig. 5 is reproduced as a dotted line. Its significance here, as implied by

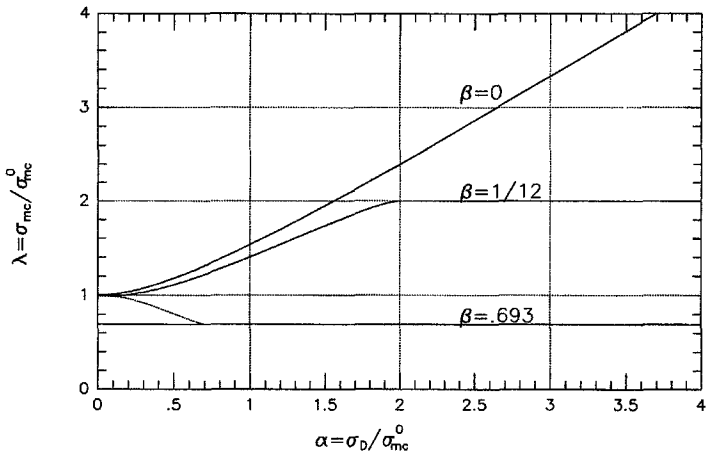

Fig. 6. Effect of debonding toughness on the matrix cracking stress; $\beta = \sigma_S/\sigma_{mc}^0$.

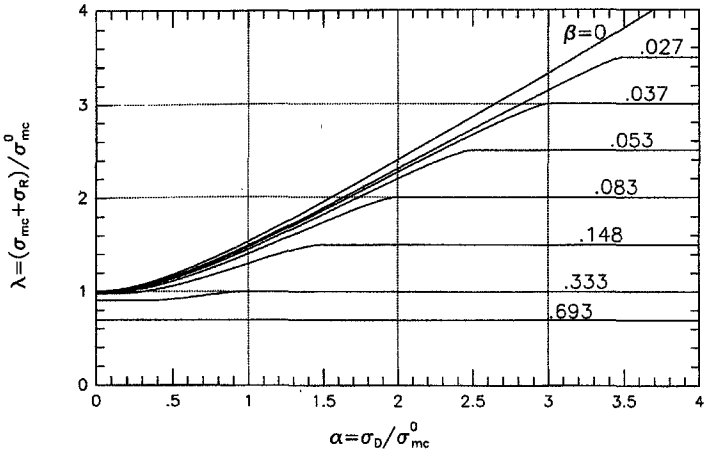

Fig. 7. Matrix cracking stress in the presence of friction, debonding toughness, and residual stress; here $\beta = \sigma_S/\sigma^0_{mc}$ and $\sigma_R = (E/E_m)\sigma^R_m$.

eqns (30) and (34a), is that for $\beta < (1/3)^{1/3}$, the value of λ stays constant between $\alpha = 0$ and the point on the dotted curve where α equals β. As illustrated by the example for $\beta = 1/12$, the ensuing variation of λ with α follows a rising trend, but must ultimately level off at the value of $\sigma_{ns}/\sigma^0_{mc}$ that corresponds to β according to eqn (31). This transition to no-slip matrix cracking is smooth but rapid, and is completed where $\lambda = \alpha$. The limiting result for $\beta = 0$ corresponds to the use of an approximate "large slip" bridging law, analogous to the one used by ACK for zero debonding energy. For the case $\beta = (1/3)^{1/3}$, we have $\lambda = (1/3)^{1/3}$ for all α.

3.5. *Effect of residual stresses*

The effects of residual stresses on matrix cracking can be taken into account easily by modifying the bridging law in the way that was explained by Marshall and Evans (1988) and Marshall and Cox (1988). If there are self-equilibrated residual stresses σ^R_f and σ^R_m in the fibers and matrix (with $c_f\sigma^R_f + c_m\sigma^R_m = 0$), then the matrix would be stress free, and the matrix crack would be closed, under the application of the far-field stress

$$\sigma_R = \left(\frac{E}{E_m}\right)\sigma^R_m. \tag{35}$$†

Hence, if the functional connection between v and σ is $v = f(\sigma)$ in the absence of residual stress, it becomes $v = f(\sigma+\sigma_R)$ for $\sigma_R \neq 0$. It follows that the complementary energy should be written as

$$Q(\sigma) = \int_{-\sigma_R}^{\sigma} v\,\mathrm{d}\sigma = \int_0^{\sigma+\sigma_R} f(\sigma+\sigma_R)\,\mathrm{d}(\sigma+\sigma_R). \tag{36}$$

Accordingly, the results of the previous sections continue to apply, with the non-dimensional stress parameter λ re-defined as

$$\lambda = \frac{\sigma_{mc}+\sigma_R}{\sigma^0_{mc}} \tag{37}$$

and now Fig. 7 shows how $\lambda \equiv \lambda(\alpha, \beta)$ varies with α for a range of values of β. Note that residual compression in the matrix ($\sigma_R < 0$) gives an increase in the matrix cracking stress. With λ re-defined by eqn (37), the results for $\lambda(0, \beta)$ that are displayed in Fig. 5 agree with those of BHE found by a quite different approach for the combined effect of only friction

†Note that σ_R is the *negative* of the quantity σ^0_R used by Marshall and Cox (1988).

and residual stress. Summing up the results, we have that the matrix cracking stress $\sigma_{mc}(\alpha, \beta)$ in the presence of friction, debonding energy and residual stress is

$$\sigma_{mc}(\alpha, \beta) = \lambda(\alpha, \beta)\sigma^0_{mc} - \sigma_R \tag{38}$$

while the matrix cracking stress in the absence of debonding energy is

$$\sigma_{mc}(0, \beta) = \lambda(0,\beta)\sigma^0_{mc} - \sigma_R. \tag{39}$$

Note that the *change* in σ_{mc} produced by the introduction of debonding energy, given by

$$\Delta\sigma_{mc} = [\lambda(\alpha,\beta) - \lambda(0,\beta)]\sigma^0_{mc} \tag{40}$$

is independent of σ_R. We remark, finally, that for sufficiently small values of the friction parameter β, the top curve in Fig. 7, corresponding to the simplified equation

$$\lambda^3 - 3\lambda\alpha^2 + 2\alpha^3 = 1 \tag{41}$$

given by eqn (34b) for $\beta = 0$, might constitute an adequate approximation up to the value of α for which λ becomes equal to $(3\beta)^{-1/2}$. Then, for still larger α, λ would be kept at this no-slip value.

3.6. *Two specific examples*

Data for two composite materials, namely silicon carbide fibers in a calcium–alumino–silicate glass ceramic matrix, and silicon carbide fibers in a silicon carbide matrix, are shown in Table 1 (Domergue *et al.*, 1994) The physical and geometric values given in the top block are nominal; in particular, the frictional resistances and the debond toughnesses have large uncertainties of 30–50%. All of the remaining quantities were calculated.

The magnitudes predicted for the increases $\Delta\sigma_{mc}$ in the matrix cracking stress that are provided by debonding energy are not insignificant. In these examples they make up for more than half of the reductions σ_R in the matrix cracking stresses that are caused by

Table 1. Data for two composite materials

material	SiC/CAS	SiC/SiC
debonding toughness $\mathcal{G}_D$ (J/m^2)	1	4
matrix toughness $\mathcal{G}_m$ (J/m^2)	25	10
matrix modulus E_m (GPa)	100	300
fiber modulus E_f (GPa)	200	200
matrix Poisson's ratio ν_m	0.2	0.2
sliding shear stress τ_S (MPa)	20	100
residual stress parameter σ_R (MPa)	120	200
fiber radius a (μm)	7	7
fiber concentration c_f	0.4	0.4
composite modulus E (GPa)	140	260
utility constant B	0.85	0.85
utility constant ρ	2.27	3.09
σ^0_{mc} (MPa)	355	325
σ_{ns} (MPa)	952	553
σ_S (MPa)	16.5	37.4
σ_D (MPa)	207	325
$\sigma_{ns}/\sigma^0_{mc}$	2.68	1.70
$\alpha = \sigma_D/\sigma^0_{mc}$	0.582	1.000
$\beta = \sigma_S/\sigma^0_{mc}$	0.046	0.115
$\lambda(\alpha,\beta)$	1.19	1.35
$\lambda(0,\beta)$	1.00	0.99
$\sigma_{mc}(\alpha,\beta)$ (MPa)	302	239
$\sigma_{mc}(0,\beta)$ (MPa)	235	122
$\Delta\sigma_{mc}$ (MPa)	67	117
$\sigma_{mc}(\alpha,\beta)/\sigma_{mc}(0,\beta)$	1.29	1.96

residual stresses. Note the *ratios* $\sigma_{mc}(\alpha, \beta)/\sigma_{mc}(0, \beta)$ of matrix cracking stresses with and without the presence of debonding energy: 1.29 for SiC/CAS and 1.96 for SiC/SiC. If residual stresses were absent, these ratios would be lower; 1.19 and 1.36, respectively.

4. TOUGHNESS AND STRENGTH

We will now estimate the effect of debonding toughness on the longitudinal strength of the aligned fiber composite when it contains a through-the-fibers crack. The strength problem has been studied in detail by Budiansky and Cui (1994) for the case of large fiber–matrix slip without debonding resistance, and it is complicated. We will limit ourselves here to consideration of very long cracks (Budiansky and Amazigo, 1989), and just assess the change in the effective, long crack composite *toughness* when debonding resistance is introduced. In addition, we will neglect the influence of the intrinsic matrix toughness in the calculation. The studies by Suo *et al.* (1993) indicate that this last approximation should be acceptable, especially since it will be made for both the cases of friction alone, and combined friction and debonding resistance, that are being compared. For the sake of clarity, we neglect residual stresses temporarily.

The energy input per unit crack advance provided by a far-field stress intensity factor K is proportional to K^2. But also, because we are neglecting the toughness of the matrix, this energy input during through-fiber crack growth must be balanced just by the crack tip bridging strain energy loss $V(c_f S)$, where S is the fiber strength and $V(\sigma)$ is the spring energy defined by

$$V(\sigma) = 2\int_0^{\sigma} \sigma \, dv(\sigma) = 2\sigma v(\sigma) - Q(\sigma). \tag{42}$$

It follows from eqns (9), (17), (26) and (27) that the strain energies V_S and V_D for fibers without and with debonding energy are

$$V_S(\sigma) = \left[\frac{a}{\sigma_A^2}\right][2\sigma_S\sigma^2] \qquad \text{for } \sigma < \sigma_S \tag{43a}$$

$$= \left[\frac{a}{\sigma_A^2}\right][4\sigma^3/3 + 2\sigma_S^3/3] \qquad \text{for } \sigma > \sigma_S \tag{43b}$$

$$V_D(\sigma) = \left[\frac{a}{\sigma_A^2}\right][2\sigma_S\sigma^2] \qquad \text{for } \sigma < \sigma_D \tag{44a}$$

$$= \left[\frac{a}{\sigma_A^2}\right][4\sigma^3/3 - 4\sigma_D^3/3 + 2\sigma_S\sigma_D^2] \qquad \text{for } \sigma > \sigma_D. \tag{44b}$$

Accordingly, for the interesting case of $c_f S > \sigma_D > \sigma_S$, the ratio $[V_D(c_f S)/V_S(c_f S)]^{1/2}$ of the corresponding long crack toughnesses K_D and K_S is

$$\frac{K_D}{K_S} = \left[\frac{1 - \left(\frac{\sigma_D}{c_f S}\right)^3 \left(1 - \frac{3\sigma_S}{2\sigma_D}\right)}{1 + \frac{1}{2}\left(\frac{\sigma_D}{c_f S}\right)^3 \left(\frac{\sigma_S}{\sigma_D}\right)}\right]^{1/2}. \tag{45}$$

For sufficiently long cracks, this is also the ratio of the composite tensile strengths with and

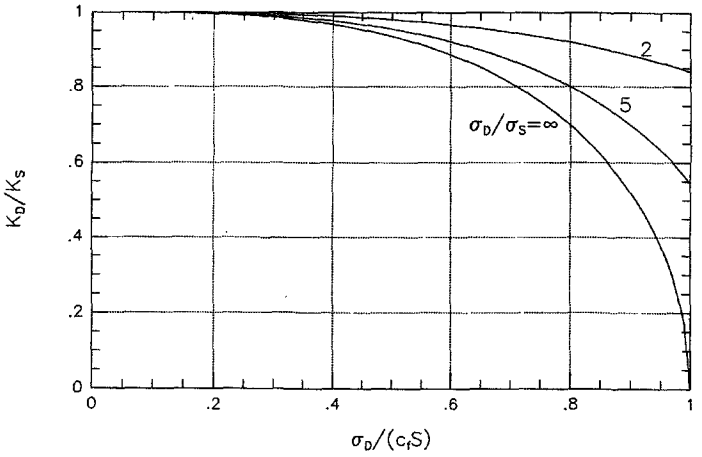

Fig. 8. Effect of debonding resistance on composite toughness.

without fiber–matrix debonding resistance. The result in eqn (42) is illustrated in Fig. 8 for $\sigma_D/\sigma_S = 2$, 5 and ∞. Toughness and strength are reduced for $\sigma_D > \sigma_S$ because debonding resistance decreases the compliance of the bridging fibers. This, in turn, increases the concentration of fiber stress at the tip of the unbridged crack.

It is unlikely that practical designs would tolerate values of $\sigma_D/(c_fS)$ anywhere near unity. We want a substantial amount of sliding to occur in the critical fibers at the crack tip before they fail in order to alleviate their stress concentration. For $\sigma_D/(c_fS)$ less than 1/2, the strength reduction due to the debonding toughness is less than 7% for all values of σ_D/σ_S. Furthermore, for cracks of finite size, the knock-down in strength would be still less than that given by eqn (45) and including the influence of matrix toughness would further alleviate the weakening effect of debonding toughness. For the examples in Table 1, with an assumed fiber strength $S = 2$ GPa, the values of K_D/K_S given by eqn (45) are 0.99 for SiC/CAS and 0.97 for SiC/SiC.

Finally, we note that residual stresses are easily taken into account by replacing c_fS in eqn (45) and in Fig. 8 by $(c_fS+\sigma_R)$, where σ_R is defined by eqn (35). The results are then valid for $(c_fS+\sigma_R) > \sigma_D > \sigma_S$. With the influence of σ_R included, the predicted values of K_D/K_S for the examples of Table 1 are even closer to unity.

5. CONCLUDING REMARKS

We have shown how to estimate the effect that a fiber–matrix interface debonding toughness has on the matrix cracking stress. In addition, an explicit formula has been presented for the approximate influence of debonding toughness on the overall composite toughness associated with large flaws. A significant finding is contained in the contrast between these two results for a practical range of parameters. Appreciable increases in the matrix cracking stress can be produced by the introduction of interfacial debonding resistance, with a negligible accompanying reduction of the overall composite toughness.

Acknowledgements—This work was partially supported by an ARPA University Research Initiative (ONR Prime Contract N00014-92-J-1808) and by the Division of Applied Sciences, Harvard University.

REFERENCES

Aveston, J., Cooper, G. A. and Kelly, A. (1971). The properties of fiber composites. In *Conference Proceedings*, National Physical Laboratory, Guildford, pp. 15–26. IPC Science and Technology Press, Teddington, U.K.

Budiansky, B. and Amazigo, J. C. (1989). Toughening by aligned, frictionally constrained fibers. *J. Mech. Phys. Solids* **37,** 93–109.

Budiansky, B. and Cui, Y. L. (1994). On the tensile strength of a fiber-reinforced ceramic composite containing a crack-like flaw. *J. Mech. Phys. Solids* **42,** 1–19.

Budiansky, B., Hutchinson, J. W. and Evans, A. G. (1986). Matrix fracture in fiber-reinforced ceramics. *J. Mech. Phys. Solids* **34,** 167–189.

Domergue, J.-M., Vagaggini, E., Evans, A. G. and Parenteau, J.-M. (1994). Relationships between hysteresis measurements and the constitutive properties of ceramic matrix composites. II : experimental studies on unidirectional materials. *J. Am. Ceram. Sci.* (in press).

Hutchinson, J. W. and Jensen, H. M. (1990). Models of fiber debonding and pullout in brittle composites with friction. *Mech. Mater.* **9,** 139–163.

Marshall, D. B. and Cox, B. N. (1988). A J-integral method for calculating steady-state matrix cracking in composites. *Mech. Mater.* **7,** 127–133.

Marshall, D. B. and Evans, A. G. (1988). The influence of residual stress on the toughness of reinforced brittle materials. *Mater. Forum.* **11,** 304–312.

McCartney, L. N. (1987). Mechanics of matrix cracking in brittle-matrix fibre-reinforced composites. *Proc. R. Soc. London* **A409,** 329–350.

Suo, Z., Ho, S. and Gong, X. (1993). Notch ductile-to-brittle transition due to localized inelastic band. *ASME J. Engr Mater. Tech.* **115,** 319–326.